Three-Dimensional Image Capture and Application V, SPIE Electronic Imaging, Proc. of SPIE 4661, San Jose, USA, Jan. 2002

3-D reconstruction of articulated objects from uncalibrated images

Fabio Remondino*, Institute of Geodesy and Photogrammetry, ETH Zürich, Switzerland

ABSTRACT

The goal of computing realistic 3-D models from image sequences is still a challenging problem. In recent years the demand for realistic reconstruction and modeling of objects and human bodies is increasing both for animation and medical applications. In this paper a system for the reconstruction of 3-D models of articulated objects, like human bodies, from uncalibrated images is presented. The scene is seen from different viewpoints and no pre-set knowledge is considered. To extract precise 3-D information from imagery, a calibration procedure must be performed. Therefore, first a camera calibration with Direct Linear Transformation (DLT) is done assuming few control points on the subject. The initial approximations of the interior and exterior orientation computed with DLT are then improved in a general photogrammetric bundle adjustment with self-calibration. Additionally a stereo matching process based on least squares matching extracts a dense set of image correspondences from the sequence. Finally a 3-D point cloud is computed by forward intersection using the calibration data and the matched points. The resulting 3-D model of human body is presented.

Keywords: 3-D reconstruction, uncalibrated images, camera calibration, least squares matching, human body modeling

1. INTRODUCTION

In recent years great progress in creating and visualizing 3-D models of scenes from image sequences has been made. Many techniques are reaching maturity and their performances are increasing very fast, even if computing realistic 3-D reconstruction of non-rigid objects from uncalibrated image sequences is still a challenging problem within many research activities. Infect recovering the geometry of a scene and the motion of the camera is a result of processes that are still quite far from being resolved and automated. The interests in 3-D object reconstruction are motivated by a wide spectrum of applications, such as video games, animations, object recognition, surveillance and visualization. There is an increasing demand for 3-D models and great attention is addressed for the visual quality of the results. The existing systems are often built around specialized hardware (e.g. laser scanner) resulting in high cost. Instead new methods [6,16,20], based on photogrammetry and computer vision, require low cost acquisition systems using only photo or video cameras. Moreover many of these applications do not require more than one camera and related software to acquire three-dimensional models of a real object.

Since many years photogrammetry deals with the extraction of high accuracy measurements from images; even if it mostly requires very precise calibration, few automated and reliable processes for close-range images are now available [6]. In the last years researchers in computer vision have tried to increase the automation of the acquisition and in particular to reduce the requirements for calibration, with the goal of automatically extract a realistic 3-D model by freely moving a camera around an object [21].

Concerning human body modeling, in the last years the demand for 3-D models has drastically increased. For animation purposes, where the shape of the human body is first defined and then animated [2,12], approximative measurements are necessary; instead for medical applications or in manufacturing industries, an exact three-dimensional measurement of the body is required [18]. The classic approaches used for building such models are laser scanner [Cyberware], structured light methods [4], infrared light scanner [17] and multi-image photogrammetry [6]. Laser scanners are quite standard in human body modeling, because of their simplicity in the use and the related market of modeling software. Structured light methods are well known and used for industrial measurement to capture the shape of parts of objects with high accuracy. Concerning the animation of the reconstructed human body, a classical computer graphics approach is the fitting of animation models to different image data, e.g. derived from image video sequences [10].

In this paper the reconstruction of 3-D models of human body from uncalibrated image sequence is described. A sequence is acquired with a digital camera, but the available information of the camera is not taken into account. The

* fabio@geod.baug.ethz.ch; phone +41-1-633 3058; fax +41-1-633 1101; http://www.photogrammetry.ethz.ch; Inst. of Geodesy and Photogrammetry, ETH-Hoenggerberg, CH-8093 Zurich, Switzerland.

images are first calibrated using DLT technique and photogrammetric self-calibrating bundle adjustment. Then image correspondences are found using a least squares matching algorithm, while the final 3-D coordinates are computed by forward intersection. As final result, a 3-D point cloud of human body is presented.

2. CAMERA CALIBRATION

Calibration and orientation of cameras and images are procedures of fundamental importance, in particular for all those applications which rely on the extraction of precise 3-D geometric information from imagery where a calibration step is as prerequisite for accurate and reliable results.
The calibration procedure is defined as the determination of geometric deviations of the physical reality from a geometrically ideal imaging system: the pinhole camera. Often, only the geometric modeling of the relation between objects and corresponding image features is considered, but a complete calibration procedure includes a more global analysis of lens system, sensor, camera electronics.
The early theories and formulations of orientation procedures were developed more than 50 years ago and today there is a great number of procedures and algorithms available. A fundamental criterion for grouping these procedures is the used camera model, i.e. the projective camera and the perspective camera model. Camera models based on perspective collineation require stable optics, not many image correspondences (min.3) and have high stability. On the other hand, projective approaches can deal with variable focal length, but are quite instables and need more parameters and image correspondences (min. 6).
A versatile and accurate photogrammetric positioning and calibration method is the bundle adjustment with self-calibration [14]. It is a global minimization of the reprojection error and was developed in the 50's and extended in the 70's. More recently, many researchers proposed new projective approaches for autocalibration (or self-calibration), in particular in the computer vision community [20]. A classical approach is based on the Kruppa equations [8], which recoveries directly the interior parameters of the camera. Other methods, based on the stratification approaches, upgrade a projective reconstruction to an Euclidean one, without solving explicitly for the intrinsic parameters of the camera. See [11] for a general overview of these different approaches.
In the next two paragraphs, photogrammetric self-calibration and Direct Linear Transformation are briefly reviewed as processes used in this work.

2.1 Photogrammetric bundle-adjustment

The mathematical basis of the self-calibrating bundle adjustment is the collinearity model; the collinearity condition states that a point in object space, its corresponding point in an image and the projective center of the camera lie on a straight line (Figure 1). The standard form of the collinearity equations is:

$$x - x_0 = -c \cdot \frac{r_{11}(X - X_0) + r_{21}(Y - Y_0) + r_{31}(Z - Z_0)}{r_{13}(X - X_0) + r_{23}(Y - Y_0) + r_{33}(Z - Z_0)} = -c \cdot \frac{U}{W}$$
$$y - y_0 = -c \cdot \frac{r_{12}(X - X_0) + r_{22}(Y - Y_0) + r_{32}(Z - Z_0)}{r_{13}(X - X_0) + r_{23}(Y - Y_0) + r_{33}(Z - Z_0)} = -c \cdot \frac{V}{W} \quad (1)$$

where:
- x, y are the image coordinates of a point P;
- x_0, y_0 are the image coordinates of the principal point PP;
- *c* is the camera constant;
- X, Y, Z are the object coordinates of a point P;
- X_0, Y_0, Z_0 are the object space coordinates of the perspective center;
- r_{ij} are the elements of the orthogonal rotation matrix R between image and object space coordinate system. R is built up with the three rotation angles (ω, ϕ, κ) of the camera.

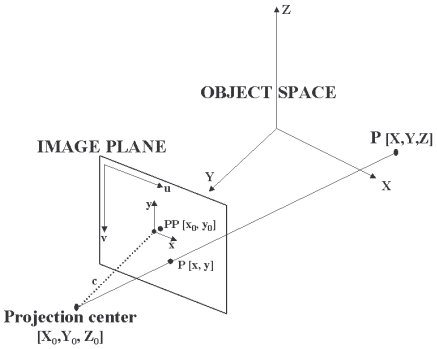

Figure 1: Used reference systems and collinearity condition

All measurements performed on digital images refer to a pixel coordinate system (u,v) while collinearity equations (1) refer to the metric image coordinate system (x,y). The conversion from pixel to image coordinates is performed with an affine pixel to image coordinate system transformation.
The collinearity model needs to be extended in order to meet the physical reality, by introducing some systematic errors; these errors are compensated with correction terms for the image coordinates, which are functions of a set of additional parameters (AP). A set of additional parameters widely used in photogrammetry [3,5] consists of the parameters of interior orientation (Δx_P, Δy_P, Δc), a scale factor for the uncertainty in pixel spacing (S_X), a shear factor (A) modelling a non-orthogonality of the image coordinate system, the parameters describing symmetrical radial lens distortion (K_1, K_2, K_3), and parameters of decentering lens distortion (P_1, P_2). The extended collinearity equations have the following form:

$$\begin{aligned} x - x_0 &= -c \cdot \frac{U}{W} + \Delta x \\ y - y_0 &= -c \cdot \frac{V}{W} + \Delta y \end{aligned} \tag{2}$$

where:

$$\begin{aligned} \Delta x &= -x_0 - \frac{\bar{x}}{c}\Delta c - \bar{x}S_x + \bar{y}A + \bar{x}r^2K_1 + \bar{x}r^4K_2 + \bar{x}r^6K_3 + (2\bar{x}^2 + r^2)P_1 + 2P_2\bar{x}\bar{y} \\ \Delta y &= -y_0 - \frac{\bar{y}}{c}\Delta c + \bar{x}A + \bar{y}r^2K_1 + \bar{y}r^4K_2 + \bar{y}r^6K_3 + +2P_1\bar{x}\bar{y} + (2\bar{y}^2 + r^2)P_2 \end{aligned} \tag{3}$$

and

$$\begin{aligned} \bar{x} &= x - x_0; \quad \bar{y} = y - y_0 \\ r &= \sqrt{\bar{x}^2 + \bar{y}^2} \end{aligned} \tag{4}$$

– K_i: parameters of symmetrical radial lens distortion
– P_i: parameters of decentering lens distortion.

Solving a self-calibrating bundle adjustment means to estimate the additional parameters in equation (3) as well as position and orientation of the camera(s) and object coordinates starting only from a set of correspondences in the images. Two collinearity equations as in (1) can be formed for each image point. Combining all equations of all points in all the images leads to a system of equations to be solved. The equations are non-linear with respect to the unknowns and, in order to solve them with a least squares method, they must be linearized, thus requiring approximations. A first order Taylor expansion is used for the linearization. Observed object coordinates are introduced via additional observation equations while geometric information in the form of additional observations (distances, angles) or geometric constraints (lines, planes) can also be used. The additional parameters are also introduced as observations. Not all additional parameters can necessarily be determined from a given arrangements of images and object points; moreover, non-determinable parameters (over-parameterisation) can lead to a degradation of the results. The resulting system of observation equations can be formulated in the Gauss-Markov model as:

$$-e = A \cdot \mathrm{x} - l \tag{5}$$

with:
– $\boldsymbol{x}^T = [\Delta X, \Delta Y, \Delta Z, \Delta X_0, \Delta Y_0, \Delta Z_0, \Delta\omega, \Delta\phi, \Delta\kappa, AP_i]$;

where:
– e is the true error;
– $\boldsymbol{A}$ is the design matrix, containing the partial derivatives of the equation (1) with respect to the unknowns, evaluated with the approximations;
– $\boldsymbol{x}$ is the vector of the unknowns;
– ΔX, ΔY, ΔZ are the changes to approximations of the object coordinates of a point
– ΔX_0 ... $\Delta\kappa$ are the changes to approximations of exterior orientation elements
– AP_i additional parameters;

– l is the absolute vector of the observations (observed minus approximated).

Calling P the weight matrix of the observations, the system is solved with the least squares solution:

$$\hat{x} = (A^T PA)^{-1} A^T Pl \tag{6}$$

Due to non linear characteristic of the problem, iterations need to be performed. The residuals v of the observations and the a posteriori variance factor σ_0 are computed as shown in (7), with r the redundancy or degree of freedom (e.g. the difference between number of equations and number of unknowns):

$$v = A \cdot \hat{x} - l \; ; \quad \hat{\sigma}_0 = \sqrt{\frac{v^T Pv}{r}} \tag{7}$$

Self-calibrating bundle adjustment is a very powerful photogrammetric calibration method. It provides for accurate orientation and location of the sensor and for accurate reconstruction of the object space. An accuracy of $1/10^{th}$ of a pixel in x,y coordinates and a depth accuracy of 1/10000 of the average object distance can be obtained. As a prerequisite, the network design requires a highly convergent imaging configuration or accurate control points information otherwise the determinability of self-calibration parameters can fail and lower accuracy is reached. For more details, see [3,9,14].

2.2 Direct Linear Transformation

The method of Direct Linear Transformation (DLT) [1] was developed in the 70's to solve the collinearity condition. The principle of DLT is to establish the relation between 3-D object coordinates and 2-D image coordinates using simpler equations. This method is suitable when the values of interior orientation (principal point and camera constant) and the parameters of exterior orientation (object space coordinates of the camera perspective center and elements of the rotation matrix R) are not available. Rearranging equation (1) leads to:

$$x = \frac{L_1 X + L_2 Y + L_3 Z + L_4}{L_9 X + L_{10} Y + L_{11} Z + 1}$$
$$y = \frac{L_5 X + L_6 Y + L_7 Z + L_8}{L_9 X + L_{10} Y + L_{11} Z + 1} \tag{8}$$

where:

$$L_1 = \frac{x_0 \cdot r_{31} - c_x \cdot r_{11}}{D}; \qquad L_2 = \frac{x_0 \cdot r_{32} - c_x \cdot r_{12}}{D}; \qquad L_3 = \frac{x_0 \cdot r_{33} - c_x \cdot r_{13}}{D};$$
$$L_4 = \frac{x_0 + c_x (r_{11} X_0 + r_{12} Y_0 + r_{13} Z_0)}{D};$$
$$L_5 = \frac{y_0 \cdot r_{31} - c_y \cdot r_{21}}{D}; \qquad L_6 = \frac{y_0 \cdot r_{32} - c_y \cdot r_{22}}{D}; \qquad L_7 = \frac{y_0 \cdot r_{33} - c_y \cdot r_{23}}{D}; \tag{9}$$
$$L_8 = \frac{y_0 + c_y \cdot (r_{21} \cdot X_0 + r_{22} \cdot Y_0 + r_{23} \cdot Z_0)}{D};$$
$$L_9 = \frac{r_{31}}{D}; \qquad L_{10} = \frac{r_{32}}{D}; \qquad L_{11} = \frac{r_{33}}{D};$$
$$D = -(r_{31} \cdot X_0 + r_{32} \cdot Y_0 + r_{33} \cdot Z_0)$$

Coefficients L_1 to L_{11}, called DLT parameters, reflect the relationship between the object space and the image plane. Equation (8) is the standard 3-D DLT equation, but the errors caused by the optical distortion of the lens can also be

included, arising the number of unknown coefficients. Equation (8) can be used for camera calibration or for 3-D coordinates computation:

1. camera calibration: the 11 unknowns of equation (8) can be determined by least squares methods, using at least 6 known points in terms of object coordinates and corresponding image coordinates (i.e. control points). A solution can be found using a least square method. Then the interior and exterior parameters of the cameras can be determined with simple and linear equations derived from equation (9).
2. 3-D coordinates computation: once the 11 parameters have been computed, 3-D coordinates of image points can be determined from equation (8) with at least 2 images.

The DLT approach yields high accuracy when control points measured with high accuracy are used. It is a direct solution that does not require initial approximations of the unknowns (as bundle adjustment requires). Therefore its results can be used as starting approximation of the unknowns for other conventional solutions.
In the literature can be found many other approaches which can be used to get the required starting approximations, in particular for the exterior orientation of the cameras [15,19,22].

3. MATCHING PROCESS AND 3-D POINT CLOUD

In order to produce a dense and robust set of corresponding image points, an automated matching process is used [7]. It establishes correspondences between three images starting from few seed points and its is based on the adaptive least squares method [13]. One image is used as template and the others as search image. The patches in the search image are modified by an affine transformation (translation, rotation, shearing and scaling) to find the correct position of the matched point. The algorithm matches corresponding points in the neighbourhood of a selected point in the search image (approximation point) by minimizing the sum of the squares differences of the grey value between the two image patches. Starting from few seed points selected in the three images, the matching process automatically determines a dense set of correspondences in the triplet. The central image is used as template and the other two (left and right) are used as search images. The matcher searches the corresponding points in the two search images independently and at the end of the process, the data sets are merged to become triplets of matched points.
To evaluate the quality of the result, different indicators are used: a posteriori standard deviation of the least squares adjustment, standard deviation of the shift in x and y directions and displacement from the start position in x and y direction. Thresholds for these values can be defined for different cases, according to the level of texture in image and to the type of template.
The least squares matching process has some problems if lacks of natural texture are presents or low resolution images are used. The performance of the process, in case of uncalibrated images, can only be improved with some local contrast enhancement of the images.
The three-dimensional coordinates of the matched points are then computed by forward intersection using the results of the calibration process. In the obtained 3-D point cloud some outliers can be present. To reduce the noise in the 3-D data and to get a more uniform density of the point cloud, a filter is applied (Figure 2). The object space is divided into boxes and the center of gravity is computed for each box. The filter can then be used in two different modes:

- to reduce the density: the points contained in each box are replaced by its center of gravity;
- to remove big outliers: if the distance between a point and the center of gravity is bigger than a threshold, the point is rejected.

Gaussian filters can also be applied to the 3-D point cloud to remove outliers and smooth the point surface. Figure 2 shows an example of thinned result after the filtering process on 3-D point cloud.

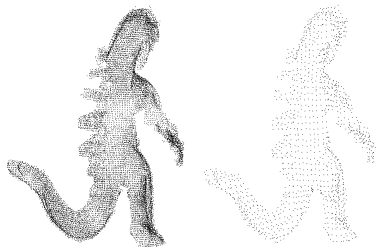

Figure 2: 3-D point cloud of an articulated object pre (left) and after (right) filtering process.

4. EXPERIMENTS AND RESULTS

The process used to compute a 3-D model from uncalibrated images is described in Figure 3.

Five images (figure 4) have been acquired with a digital still-video camera SONY DSC-F505 Cybershot. No information

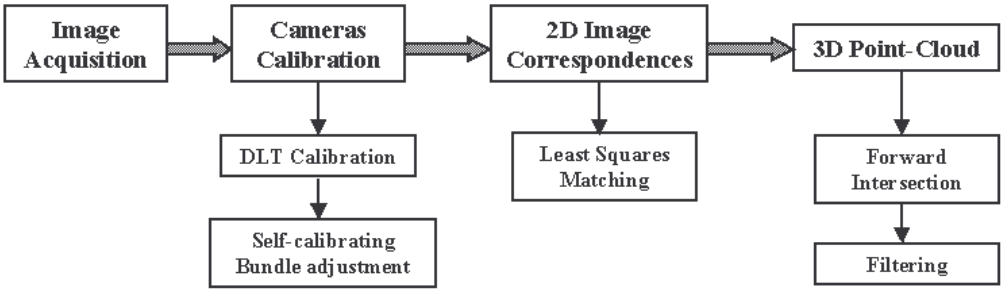

Figure 3: Graphical representation of the process

regarding the camera parameters was taken into consideration. The camera focus and zoom were fixed during the acquisition and for the process, a square pixel size of 0.008 mm and the principal point fix in the middle of the images were supposed.

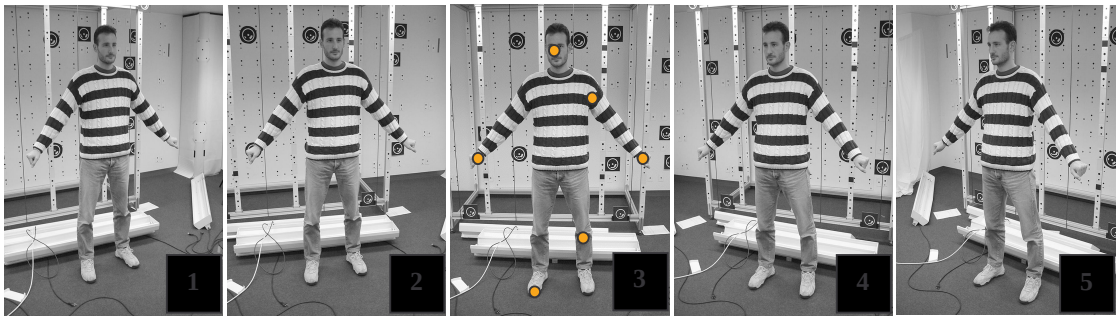

Figure 4: Sequence of images used for the experiment. In image nr.3, the measured control points used for DLT calibration are visualized.

As first step, DLT calibration was performed. Six control points were measured manually on the body. The corresponding image points were selected in the middle image (figure 4, image nr.3) and the correspondences matched in the other frames using least squares matching. The DLT parameters were computed for all the images and a first approximation of the camera parameters (interior and exterior orientation) was obtained. These values were used as starting approximations for the bundle adjustment. The self-calibration was run as a free-network adjustment (no control points information was used) and the 3-D datum was imported from the DLT results. Some other image correspondences measured manually on the testfield in the background and on the human body were also used as tie points for the adjustment. A total of 33 object points observations were imported in the bundle. At the end of the process, a camera constant of 9.1 mm was estimated while the correct position of the principal point could not be determined because no camera roll diversity was present. Concerning the lens distortion parameters, only the first two parameters of radial distortion (K_1 and K_2) could be computed, as an over-parameterization could lead to a degradation of the results. Figure 5 shows the global distortion of the camera due to the systematic errors, computed with model equation (2). Each point of the regular grid was distorted with the achieved additional parameters and then amplified in both directions for a better visualization.

The final a posteriori standard deviation of image coordinates was 0.04 mm while the theoretical precision of the observations was σ_{XY} = 8mm and σ_Z = 15mm. The final configuration of the system after the bundle adjustment is shown in Figure 6.

To reconstruct the human body model, image correspondences were found as explained in section 3, using two triplets of images (1-2-3 and 3-4-5) and matching the area of interest every 2 pixels. An average of 25000 points per couple of images was matched. The 3-D coordinates of the matched points were then computed by forward intersection using the calibration and orientation data. This process achieved a mean accuracy of 7 mm in xy plane and 14 mm in z direction.

The process was performed independently for the 2 triplets and the results merged together into a cloud of about 50000 points. The filtering process reduced the amount of redundant data (overlapping data sets) to a more uniform and thinned

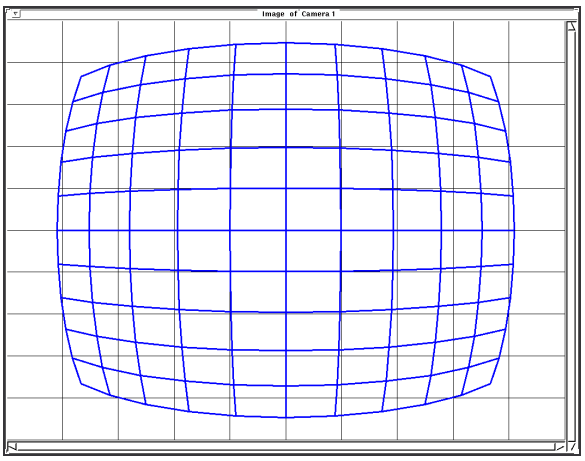

Figure 5: Global distortion of the images computed with extended collinearity equations (2)

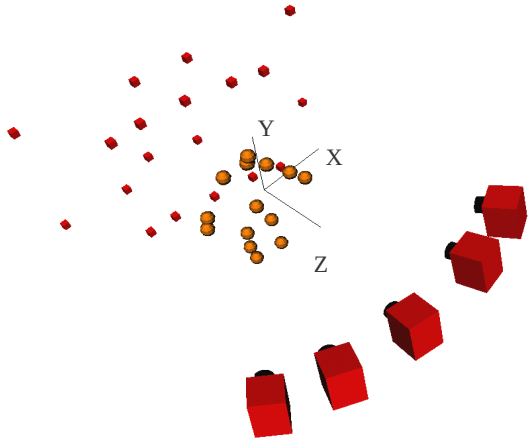

Figure 6: Achieved configuration after the bundle adjustment

density of the points. Figure 7 shows the point cloud of the human body after the filtering process (ca. 15000 points) from different views. The filtering process did not always succeed in removing outliers, therefore some manual editing was required. Some peaks and discontinuities contained in the created point cloud represent measuring errors. The causes could be in the matching process as it fails in areas with low texture; problems of the process occurred also in places where big differences between the template and the search images are present. This is due to the convergent arrangement of the acquisition process and to the topology of the human body. As example, the shape of the trousers near the knees does not facilitate the matching process as many shadows and folds are present. Moreover the acquisition process lasted ca. 1 minute and a small movement of the person during this time can not be excluded.

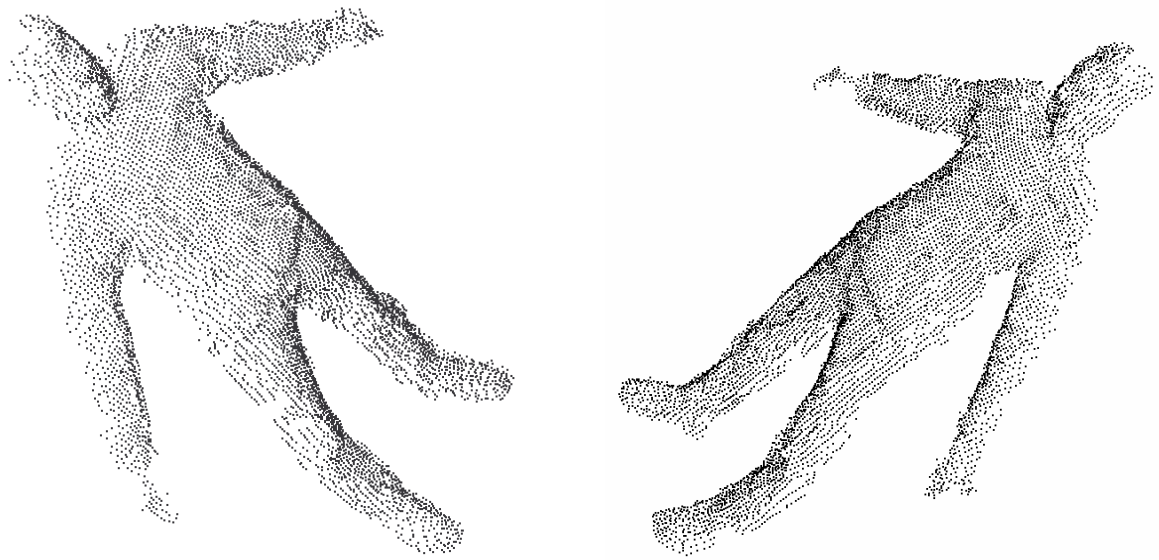

Figure 7: 3-D point cloud of human body

5. CONCLUSIONS

In this paper a low-cost system used to create 3-D model of human body was described. A photogrammetric approach was chosen among others for its versatility and accuracy. Uncalibrated images were used and the final calibration process

achieved a posteriori standard deviation of image coordinates of 0.04 mm (5 times the pixel size). Preliminary results of the 3-D reconstruction were presented and the main problems discussed, in particular for the matching process. A 3-D point cloud of human body could be computed and a mean accuracy of 7 mm in xy plane and 14 mm in z direction was achieved. The presented results of human model cannot be compared with results obtained using laser scanning but improving the described approach more accurate models can be obtained. The 3-D point cloud of Figure 7 is very dense in almost all regions but the generation of a surface model starting from unorganized 3-D point cloud requires non-standard procedures which can be found in commercial software. A standard 2.5 Delauney triangulation can not create a meshed surface from the obtained 3-D point cloud.

In the future, more and closer images could be selected to improve the network configuration, in particular for the matching process. As the bundle adjustment requires very good starting approximation, in particular for the exterior orientation of the cameras, commercial photogrammetric software (PhotoModeler, Australis) could also be used to obtain the necessary orientation data. It is also planned to complete the reconstruction of the human body acquiring images all around the object.

ACKNOWLEDGEMENT

I would like to thank Nicola D'Apuzzo, who works with me at the Institute of Geodesy and Photogrammetry at ETH Zurich, for providing me with his software for visualization and editing of a 3-D point cloud.

REFERENCES

1. Abdel-Aziz, Y.I., & Karara, H.M., "Direct Linear Transformation from comparator coordinates into object space coordinates in close-range photogrammetry", *Proceedings of the ASP Symposium on Close-Range Photogrammetry*, pp. 1-18, 1971
2. Badler N. I., Palmer O., Bindiganavale R., "Animation Control for Real Time Virtual Humans", *Comm. ACM*, **42 (8)**, pp. 65-73, 1999
3. Beyer, H.A., "Geometric and Radiometric Analysis of CCD-Cameras. Based Photogrammetric Close-Range system", Ph.D. thesis **51**, IGP ETH Zurich, pp.186, 1992
4. Bhatia G., Smith K. E., et al., "Design of a Multisensor Optical Surface Scanner", *Sensor Fusion VII, SPIE Proc.* **2355**, pp. 262-273, 1994
5. Brown, D.C., "Close-range Camera Calibration", *Photogrammetric Engineering and Remote Sensing* **37(8)**, pp.855-866, 1971
6. D'Apuzzo N., "Automated Photogrammetric Measurement of Human Faces", *Int. Archives of Photogrammetry and Remote Sensing* **32(B5)**, Hakodate, Japan, pp. 402-407, 1998
7. D'Apuzzo N., Plänkers R., "Human Body Modeling from Video Sequences", *Int. Archives of Photogrammetry and Remote Sensing* **32**, Onuma, Japan, pp. 133-140, 1999
8. Faugeras O., Luong Q.T., Maybank S., "Camera Self-calibration: Theory and Experiments", *Computer Vision - ECCV92, Lecture Notes in Computer Science* **588**, Springer-Verlag, pp. 321-334, 1992
9. Fraser, C.S., "Digital Camera Self-calibration", *ISPRS Journal of Photogrammetry and Remote Sensing* **52**, pp. 149-159, 1997
10. Fua, P., Gruen, A., et al., "Human body Modeling and Motion Analysis from Video Sequences", *Int. Symposium on Real Time Imaging and Dynamic Analysis*, June 2-5, Hokadate, Japan, 1998
11. Fusiello, A, "Uncalibrated Euclidean Reconstruction: a review", *Image and Vision Computing* **18**, pp. 555-563, 2000
12. Gavrila D. M., Davis. L., "3-D model-based tracking of humans in action: a multi-view approach", *Proc. Conference on Computer Vision and Pattern Recognition*, San Francisco, CA, USA, pp. 73-80, 1996
13. Grün A., "Adaptive least squares correlation: a powerful image matching technique", *South African Journal of Photogrammetry, Remote Sensing and Cartography* **14(3)**, pp. 175-187, 1985
14. Grün A., Beyer, H.A,. "System calibration through self-calibration", in *Calibration and Orientation of Cameras in Computer Vision, Springer Series in Information Sciences* **34**, Eds.: Grün, Huang., 2001
15. Haralick, R.M., Lee, C., et al., "Analysis an solution of the three point perspective pose estimation problem", *Proc. IEEE Conf. On Computer Vision and Patter Recognition*, pp.592-598, 1991

16. Hartley, R., Zissermann, A., "Multi-View Geometry in Computer Vision", Cambridge University Press, pp. 607, 2000
17. Horiguchi C., "Body Line Scanner. The development of a new 3-D measurement and Reconstruction system", *Int. Archives of Photogrammetry and Remote Sensing* **32(B5)**, Hakodate, Japan, pp. 421-429, 1998
18. McKenna P., "Measuring Up", *Magazine of America's Air Force* **XL(2)**, 1996
19. Or S.H, Luk W.S., et al., "An efficient iterative pose estimation algorithm", *Image and Vision Computing Journal*, 16(5) , pp.355-364, 1998
20. Pollefeys, M, "Self-calibration and metric 3-D reconstruction from uncalibrated image sequences", Ph.D. thesis, K.U. Leuven, Belgium, 1999
21. Pollefeys, M., "Tutorial on 3-D modeling from images", *Tutorial at ECCV2000*, Dublin, Ireland, 2000
22. Quan L., Lan, Z., "Linear N-point Camera Pose Determination", *IEEE Transaction on Pattern Analysis and Machine Intelligence*, **21(7)**, 1999

Cyberware: http://www.cyberware.com [15 December 2001]

PhotoModeler: http://www.photmodeler.com [15 December 2001]